157. Nucleic-Acid Analogs with Restricted Conformational Flexibility in the Sugar-Phosphate Backbone ('Bicyclo-DNA')

Part 5[1])

Synthesis, Characterization, and Pairing Properties of Oligo-α-D-(bicyclodeoxynucleotides) of the Bases Adenine and Thymine (α-Bicyclo-DNA)[2])

by **Martin Bolli**[3]), **Paolo Lubini**[4]), and **Christian Leumann***

Institut für Organische Chemie der Universität, Freiestrasse 3, CH–3012 Bern

Dedicated to Professor *A. Eschenmoser* on the occasion of his 70th birthday

(9.X.95)

A conformational analysis of the (3′*S*,5′*R*)-2′-deoxy-3′,5′-ethano-α-D-ribonucleosides (α-D-bicyclodeoxynucleosides) based on the X-ray analysis of N^4-benzoyl-α-D-(bicyclodeoxycytidine) **6** and on ^{1}H-NMR analysis of the α-D-bicyclodeoxynucleoside derivatives **1**–**7** reveals a rigid sugar structure with the furanose units in the 1′-*exo*/2′-*endo* conformation and the secondary OH groups on the carbocyclic ring in the pseudoequatorial orientation. Oligonucleotides consisting of α-D-bicyclothymidine and α-D-bicyclodeoxyadenosine were successfully synthesized from the corresponding nucleosides by phosphoramidite methodology on a DNA synthesizer. An evaluation of their pairing properties with complementary natural RNA and DNA by means of UV/melting curves and CD spectroscopy show the following characteristics: *i*) α-bcd(A_{10}) and α-bcd(T_{10}) (α = short form of α-D) efficiently form complexes with complementary natural DNA and RNA. The stability of these hybrids is comparable or slightly lower as those with natural β-d(A_{10}) or β-d(T_{10}) (β = short form of β-D). *ii*) The strand orientation in α-bicyclo-DNA/β-DNA duplexes is parallel as was deduced from UV/melting curves of decamers with nonsymmetric base sequences. *iii*) CD Spectroscopy shows significant structural differences between α-bicyclo-DNA/β-DNA duplexes compared to α-DNA/β-DNA duplexes. Furthermore, α-bicyclo-DNA is *ca.* 100-fold more resistant to the enzyme snake-venom phosphodiesterase with respect to β-DNA and about equally resistant as α-DNA.

1. Introduction. – One of the first DNA analogs to be synthesized and its pairing properties with the natural nucleic acids being characterized was α-DNA[5]), composed of 2′-deoxy-α-D-ribonucleosides. Based on model building, *Séquin* reported more than 20 years ago on the possibility of right-handed *Watson-Crick* duplex formation between an

[1]) Part 4: [1].

[2]) Preliminary communication on α-Bicyclo-DNA: [2].

[3]) Part of the Ph. D. thesis of *M. B.* [3]. Current address: Laboratorium für Organische Chemie, ETH-Zentrum, Universitätstrasse 16, CH–8092 Zürich.

[4]) Laboratorium für Organische Chemie, ETH-Zentrum, Universitätstrasse 16, CH–8092 Zürich. Current address: Institut für anorganische Chemie der Universität, Tammannstrasse 4, D–37077 Göttingen.

[5]) In α-DNA, α-bicyclo-DNA, α-bdc(A_{10}), β-bdc(T_{10}), β-d(T_{10}) *etc.*, α and β refer to the configuration at the anomeric center and are used as short forms of the anomeric prefixes α-D and β-D, respectively.

α-D-oligonucleotide and either a parallel oriented β-D-complement or an antiparallel oriented α-D-complement [4], this well before efficient methods for oligonucleotide synthesis came to age. Meanwhile, both structural predictions were verified by 2D-NMR techniques on mixed α-D-, β-D-oligomer duplexes [5] [6], and on a purely α-D-anomeric hexamer duplex [7]. Furthermore, it was shown that the base-pairing efficiency of α-DNA to complementary α- or β-DNA is comparable to that of natural duplexes exhibiting similar values for duplex-formation enthalpy (ΔH) and entropy (ΔS) [8]. α-DNA also pairs to complementary RNA [9], is generally more stable towards enzymatic degradation by nucleases [10], but does not induce RNase H activity [9] [11]. Homopyrimidine α-DNA strands also bind to β-DNA duplexes forming triple helices. α-D-Oligothymidine sequences thereby prefer parallel strand alignment with reversed *Hoogsteen* base-pair formation, whereas mixed (cytosine- and thymine-containing) oligomers bind in the antiparallel orientation forming *Hoogsteen* base pairs [12].

In our laboratory, we recently designed and synthesized bicyclo-DNA, an oligonucleotide analog with a rigid sugar substitute, in an effort to explore the effect of conformational restriction (and thus preorganization) of oligonucleotide single strands onto complex formation with natural DNA and RNA. While our previous focus was on the synthesis and characterization of bicyclo-DNA of the natural β-D-configuration [1] [3] [13–17] (*i.e.* β-bicyclo-DNA[5])), it was now clearly of interest to explore the properties of α-bicyclo-DNA[5]) (*Fig. 1*). Here, we wish to report on the conformational properties of α-D-bicyclodeoxynucleosides as well as on the pairing properties and the nuclease resistance of oligomers thereof containing the bases adenine and thymine. The synthesis of the corresponding α-D-bicyclodeoxynucleosides has been already described [13].

2. Conformation of α-D-Bicyclodeoxynucleosides. – 2.1. *X-Ray Structure of* N[4]*-Benzoyl-α-*D*-(bicyclodeoxycytidine)* **6**[6]). To obtain insight into the conformational character-

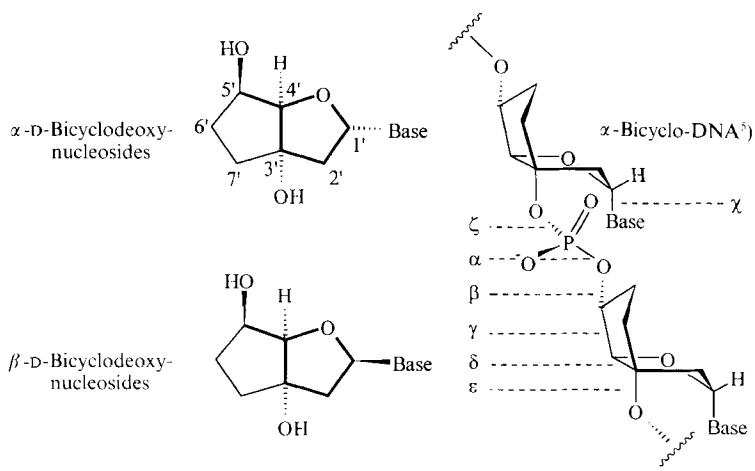

Fig. 1. *Structure of* α-D- *and* β-D-*bicyclodeoxynucleosides and* α-*bicyclo-DNA with backbone torsion angles*

[6]) Crystal data and coordinates were deposited with the *Cambridge Crystallographic Data Centre.*

istics of the α-D-bicyclodeoxynucleosides, we chose **6** as a candidate for X-ray structure determination (*Fig. 2*, selected torsion angles are given in *Table 1*). Crystals of this α-D-cytidine analog contain two independent molecules A and B in their asymmetric unit. Essentially, A and B differ from each other in the ring pucker of the furanose unit. In molecule A (*Fig. 2a*), the furanose part occurs in the 1′-*exo* conformation (pseudorotation phase angle $P = 129.7°$), while in B (*Fig. 2b*) an almost perfect 2′-*endo* conformation ($P = 159.1°$) is observed. In both molecules A and B, the secondary OH group on the carbocyclic ring occupies the pseudoequatorial position, giving rise to torsion angle γ of 146.7° and 133.9°, respectively. Torsion angle χ, defining the conformation around the nucleosidic bond, adopts values around 170° in both forms. Thus, the base substituent is oriented in the '*anti*' range with its base-pairing side pointing away from the sugar unit. As a consequence of the 1′-*exo* and 2′-*endo* conformation in A and B, O(3′) of the sugar and N(1) of the base are brought into close *van der Waals* distance (d(O(3′)–N(1)) = 3.24 Å in A and 3.27 Å in B)[7]. Within the unit cell, the two molecules A and B are connected by one intermolecular H-bond between O(3′) of conformer A and H–O(5′) of molecule B (*Fig. 2c*). H-Bonds between sugar and base residues exist between molecules A *and* B (O(3′)–H···O(2)) as well as *within* molecules A and B (N(4)–H···O(5′)). No H-bonds between the nucleobases were detected.

2.2. *Solution Structure of* α-D-*Bicyclodeoxynucleosides.* Additional information on the preferred conformation of the α-D-bicyclodeoxynucleoside derivatives **1**–**7** was obtained by H,H coupling-constant analysis in the corresponding ^{1}H-NMR spectra. The relevant data are summarized in *Table 2*. It becomes clear that the vicinal coupling constants between the protons at C(1′) and C(2′) as well as C(4′) and C(5′) in **1**–**7** are almost invariant, indicating that the bicyclic core conformation is insensitive towards the nature of the bases attached to it. Because of the absence of a proton at C(3′), we cannot assign the complete sugar pucker of the furanose unit. However, using the modified *Karplus* relation of *Davies* [18], values for the dihedral angles ν_1 (24–32°) and γ (133–135°) could be obtained. These values are in excellent agreement with those obtained from the X-ray analysis of **6** and further underline the conformational rigidity of the bicyclonucleosides.

Table 1. *Torsion Angles Relevant in DNA Backbone Conformation for* N^4-*Benzoyl-*α-D-*bicyclodeoxycytidine* **6** (two independent molecules A and B)

Torsion angles	A	B
γ (O(5′)–C(5′)–C(4′)–C(3′))	146.7	133.9
δ (C(5′)–C(4′)–C(3′)–O(3′))	124.5	136.2
χ (O(4′)–C(1′)–N(1)–C(2))	172.5	169.1
ν_0 (C(4′)–O(4′)–C(1′)–C(2′))	–32.0	–18.7
ν_1 (O(4′)–C(1′)–C(2′)–C(3′))	32.7	28.8
ν_2 (C(1′)–C(2′)–C(3′)–C(4′))	–21.4	–26.9
ν_3 (C(2′)–C(3′)–C(4′)–O(4′))	3.3	16.9
ν_4 (C(3′)–C(4′)–O(4′)–C(1′))	18.0	1.0

[7]) Interestingly, the benzamide unit in both molecules A and B is not coplanar with the cytosine ring. Maximum deviation occurs in A with a torsion of 18° around the C(4)–N(4) bond.

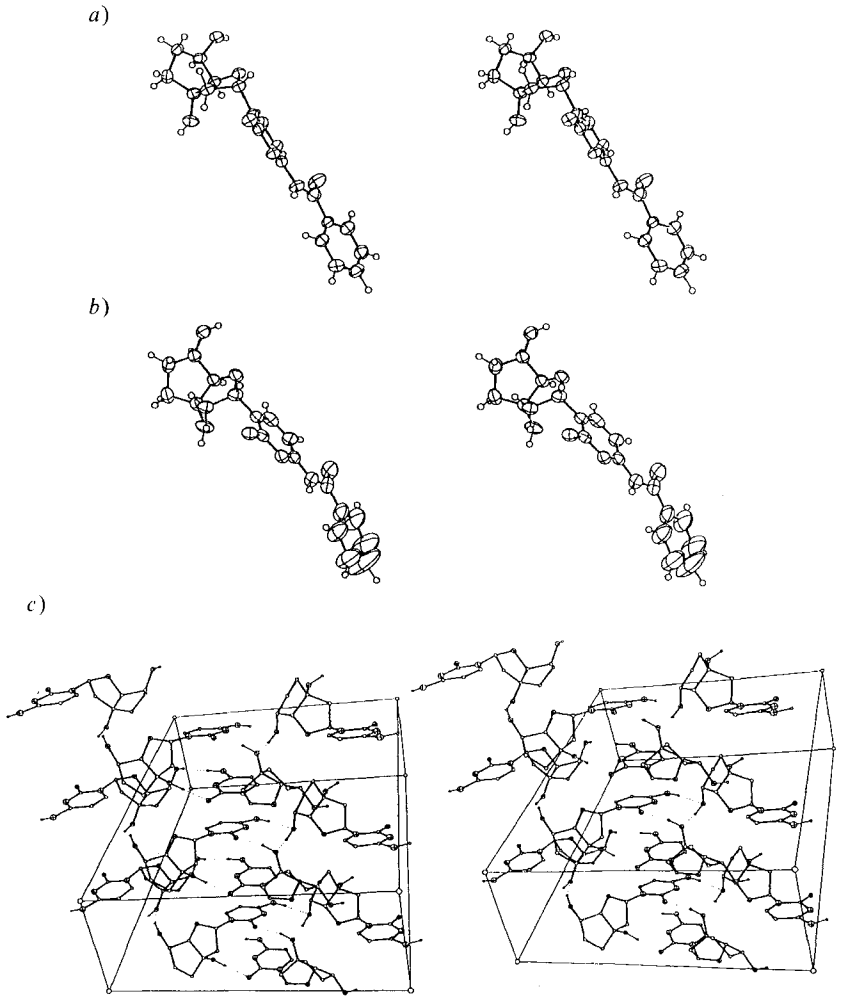

Fig. 2. *X-Ray structure of* **6**: a) b) *ORTEP plots* (stereoscopic views) *of the two independent molecules A and B in the asymmetric unit and* c) *crystal packing*

The 2′-deoxy-α-D-ribonucleosides in α-D-oligonucleotide duplexes [6] as well as in their mononucleoside form preferably occur in the 3′-*exo* sugar pucker and thus are conformationally related to their β-D-epimers (*Fig. 3*). In the case of the bicyclodeoxynucleosides, both the α-D- and β-D-series [13] prefer the same type of furanose conformation (1′-*exo*,2′-*endo*) irrespective of the configuration at the anomeric center (*Fig. 3*). As a consequence, α-D- and β-D-bicyclonucleosides mimick the backbone torsion angle δ of the natural α-D- and β-D-deoxyribonucleosides very well. However, it should be noted that there are considerable differences within the backbone angle γ. In duplexes of α- and β-DNA, γ always adopts the *gauche* conformation. In contrast to this, α-D- and β-D-bicyclodeoxynucleosides strongly prefer the antiparallel arrangement (*Fig. 3*).

Table 2. *Selected δ and J Values from ^{1}H-NMR Spectra of Compounds* **1–7**

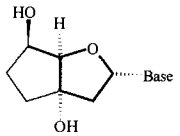

1 Base = Thy
2 Base = Ade
3 Base = Cyt
4 Base = Gua
5 Base = BZ^{6}Ade
6 Base = Bz^{4}Cyt
7 Base = Ib^{2}Gua

	δ [ppm]				J [Hz]		
	H–C(1′)	H_α–C(2′)	H_β–(C2′)	H–C(4′)	^3J(1′,2′α)	^3J(1′,2′β)	^3J(4′,5′)
1 (D_2O)	6.15	2.38	2.58	4.37	7.0	4.3	5.3
2 (D_2O)	6.32		2.71–2.80	4.32	6.1	3.9	5.2
3 (CD_3OD)	6.20	2.29	2.57	4.36	7.1	3.6	5.2
4 ((D_6)DMSO)	6.17	2.48	2.52	4.09	6.4	4.3	4.9
5 (CD_3OD)	6.63	2.84	2.75	4.35	7.4	2.5	5.0
6 (CD_3OD)	6.23	2.40	2.65	4.51	7.0	2.6	5.2
7 (CD_3OD)	6.42	2.74	2.65	4.34	7.1	2.8	5.2

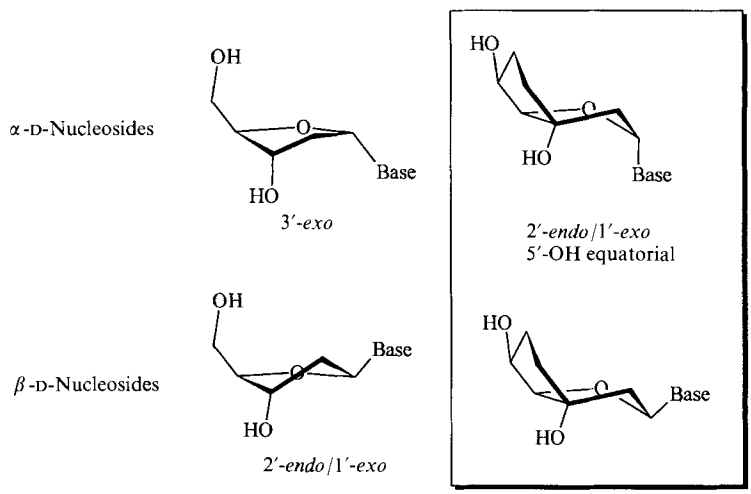

Fig. 3. *Preferred conformations of α-D- and β-D-deoxyribonucleosides, and of α-D- and β-D-bicyclodeoxynucleosides*

3. Synthesis of α-D-Oligo(bicyclodeoxynucleotides). – 3.1. *Synthesis of Building Blocks.* The automated synthesis of α-bicyclo-DNA oligomers was planned in analogy to that in the β-D-series [15] on the basis of phosphoramidite methodology. For phosphoester protection, the allyl group, introduced into oligonucleotide synthesis by *Hayakawa et al.* [19], was chosen. The synthesis of the corresponding phosphoramidite building blocks **10** and **11** *via* the tritylated intermediates **8** and **9**, respectively, as well as of the nucleoside-substituted solid supports *via* the activated esters **12** and **13** (*Scheme 1*), respectively, proceeded with similar ease and efficiency as in the β-D-bicyclo series, rewarding us with sufficient material to tackle the problem of oligomer synthesis.

Scheme 1

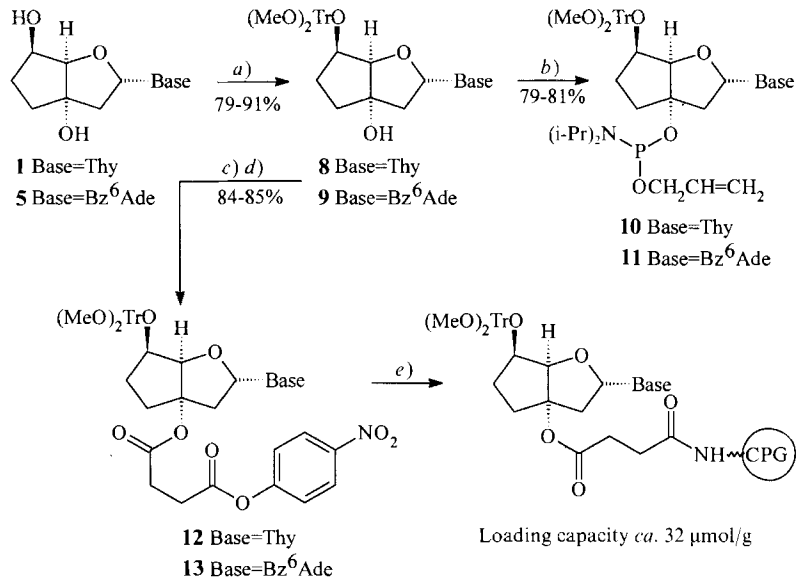

a) $[(MeO)_2Tr]CF_3SO_3$, py. *b*) $(CH_2{=}CHCH_2O)[(i\text{-}Pr)_2N]PCl$, $(i\text{-}Pr)_2NEt$, THF. *c*) Succinic anhydride, py, $4\text{-}(Me_2N)C_5H_4N$. *d*) 4-Nitrophenol, dioxane, DCC. *e*) LCAA-CPG, dioxane, Et_3N.

3.2. *Oligomer Synthesis.* α-D-Oligo(bicyclodeoxynucleotides) were synthesized on a *Pharmacia-Gene-Assembler-Special* DNA synthesizer on the 1.3-μmol scale. Solvents, reagents, and phosphoramidite concentrations were identical to those used for natural DNA synthesis. The standard automatic cycle was changed as to permit a slightly extended detritylation time and a coupling time of six min (*Scheme 2*). Coupling yields, determined by trityl assay were generally > 95%. Every chain assembly was terminated with the removal of the last trityl group (trityl-off mode). Palladium(0)-catalyzed allyl deprotection [19] followed by detachment from the solid support (and removal of base protecting groups where necessary) with conc. NH_3 afforded the crude oligomers that were further purified by HPLC and analyzed by gel-capillary electrophoresis (GCE) as well as by MALDI-TOF mass spectrometry.

With this protocol, the four α-D-bicyclodeoxynucleotide sequences, α-bcd(A_{10}), α-bcd(T_{10}), α-bcd(T_{20}), and α-bcd(T-T-A-A-A-T-T-A-T-A) (*Scheme 2*), used in the following biophysical experiments were obtained in overall yields of 18–28% (bcd denotes *bic*yclo*d*eoxynucleoside residue). The HPLC trace of the crude synthesis product α-bcd(A_{10}) (*Fig. 4, a*), as a representative example, underlines the efficiency of the synthesis. *Fig. 5* shows electropherograms of purified 10- and 20-mers (top) and the corresponding MALDI-TOF mass spectra (bottom) impressively demonstrating the high quality and the consistency of the isolated material. Although having phosphodiester linkages to tertiary alkoxy groups, the α-D-oligo(bicyclodeoxynucleotides), as their β-D-analogs, are

Scheme 2

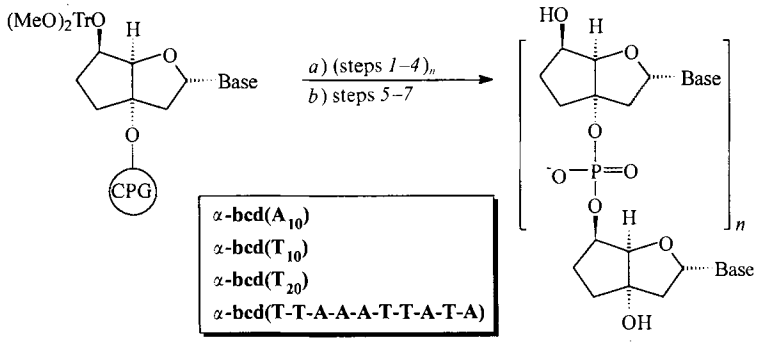

Synthesis cycle (1.3 μmol)	
Chain assembly	
1) detritylation	3% $CHCl_2COOH$ in CH_2ClCH_2Cl, 60 s
2) coupling	0.1M phosphoramidite (11 equiv.), 0.5M 1*H*-tetrazole (139 equiv.) in MeCN (6 min)
3) capping	3% 4-(dimethylamino)pyridine, 10% Ac_2O, 15% 2,4,6-trimethylpyridine in MeCN (0.8 min)
4) oxidation	0.01M I_2 in 2,4,6-trimethylpyridine/H_2O/MeCN 1:6:11 (18 s)
Deprotection/detachment	
5) detritylation	as *1*)
6) phosphate deprotection	2.5 equiv. of tris(dibenzylideneacetone)dipalladium(0), PPh_3 (25 equiv.) per allyl group, in THF (2 ml), $BuNH_2$ (240 μl), HCOOH (90 μl), 55°, 90 min
7) base deprotection detachment	conc. NH_3 (3 ml), 55°, 16 h

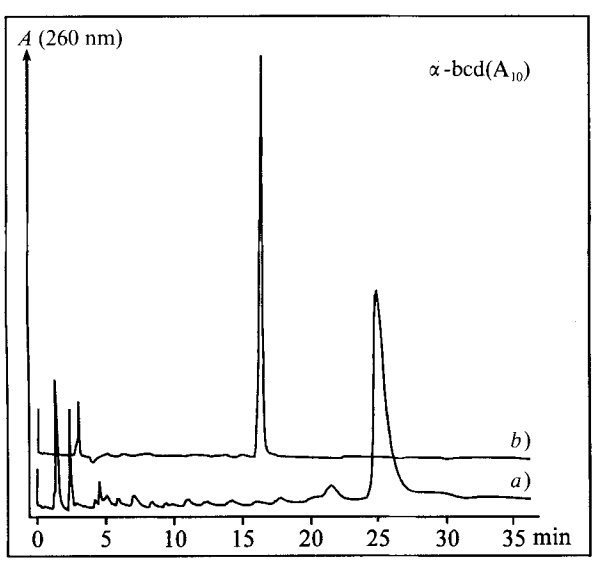

Fig. 4. *HPLC Traces of α-bcd(A10):* a) *crude synthesis product (DEAE) and* b) *control injection after purification* (reversed-phase). For details, see *Exper. Part.*

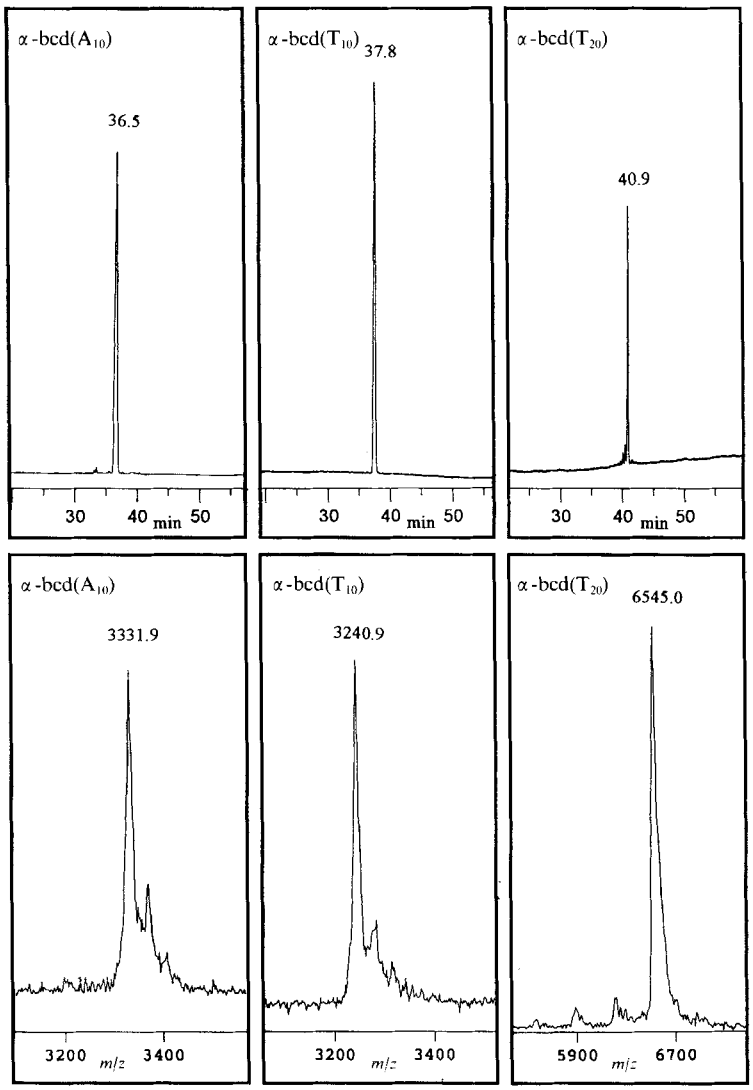

Fig. 5. *Electropherograms* (top) *and MALDI-TOF mass spectra* (bottom) *of the* α-D-*oligo(bicyclodeoxynucleotides)* α-*bcd*(A_{10}), α-*bcd*(T_{10}), *and* α-*bcd*(T_{20})

chemically stable and show no signs of degradation (HPLC control) under the conditions used for the investigation of their pairing properties (*e.g.* melting curves).

4. Pairing Properties of α-Bicyclo-DNA. – 4.1. *With Itself.* There exist considerable differences in the modes of association between homothymidine sequences of α- and β-DNA. We found earlier that an oligomer of α-D-thymidine, 20 nucleotides in length, in contrast to its natural β-D-isomer, forms an antiparallel oriented monomolecular hairpin

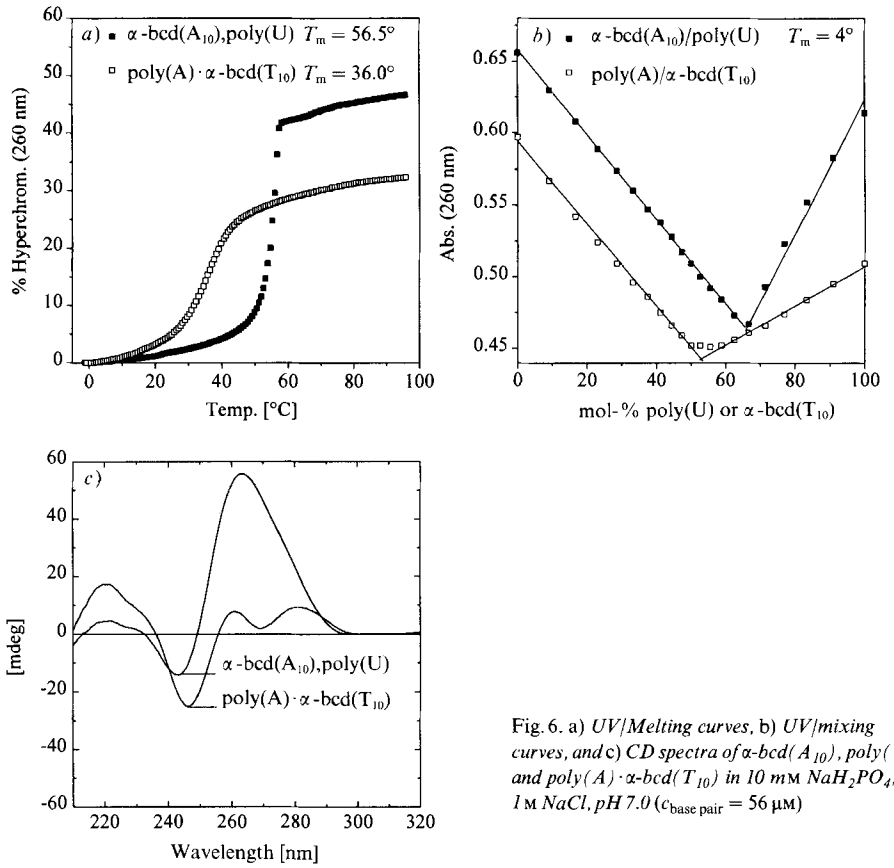

Fig. 6. a) *UV/Melting curves*, b) *UV/mixing curves, and* c) *CD spectra of α-bcd(A_{10}), poly(U) and poly(A)·α-bcd(T_{10}) in 10 mM NaH_2PO_4, 1 M NaCl, pH 7.0* ($c_{base\ pair}$ = 56 μM)

duplex with T·T base pairs in the stem [20]. We, therefore, investigated whether duplex formation does also occur in the case of its bicyclic analogue α-bcd(T_{20}). UV/Melting curves of α-bcd(T_{20}) at different wavelengths, however, did not show any signs of a cooperative structural transition (data not shown). As expected, also oligo-α-bcd(A) sequences did not show any structural transitions related to duplex melting at neutral pH (UV/melting curves not shown).

4.2. *With Complementary RNA.* α-bcd(T) and α-bcd(A) sequences readily form complexes with poly(U) and poly(A) as determined by UV/melting curves (1M NaCl) of 1:1 mixtures poly(A)/α-bcd(T_{10}) and α-bcd(A_{10})/poly(U) (*Fig. 6, a*) with corresponding T_m values of 36° in the former and 56.5° in the latter case. Under these conditions, the thermal stability of the complex α-bcd(A_{10}), poly(U) is equal to that of β-d(A_{10}), poly(U) but by *ca.* 14° less stable than that of β-bcd(A_{10}), poly(U) (T_m = 70°). Interestingly, the duplexes between poly(A) and β-d(T_{10}), α-bcd(T_{10}), and β-bcd(T_{10}) are very similar in thermodynamic stability (ΔT_m = 2 °C).

The stoichiometry of complex formation in the α-bicyclo-DNA/RNA hybrids was investigated by the method of continuous concentration variation [21]. The UV/mixing

curve of poly(A)/α-bcd(T_{10}) shows two straight lines with an intersection point near 50 mol-% α-bcd(T_{10}) (base ratio) indicating only duplex formation (*Fig. 6, b*) taking place. The mixing curve of the alternative hybrid α-bcd(A_{10})/poly(U) also shows two straight lines, the intersection point of them, however, being at 67 mol-% poly(U) (base ratio), indicating triplex formation of the U·A·U type. Higher-order complex formation in the latter case *vs.* duplex formation in the former case can be explained in terms of an entropic advantage of the poly(U)/oligo(A) systems (bimolecular triplexes). However, we note that with α-bcd(A_{10}) as well as with β-d(A_{10}), triplex formation with poly(U) at 1M NaCl is independent of the stoichiometric base ratio (α-bcdA/U or β-dA/U), whereas with β-bcd(A_{10}) a base ratio 1:2 (β-bcd/A/U) is required [15].

CD Spectra of both bicyclo-DNA/RNA complexes (*Fig. 6, c*) are seemingly different from each other, the triplex α-bcd(A_{10})·2poly(U) showing the most intense ellipticity. The spectrum of the duplex poly(A)·α-bcdT_{10} exhibits appreciable similarities to the spectra of poly(A), β-d(T_{10}) but is quite different from that of poly(A), α-d(T_8) [22]. The differences are mainly located at wavelengths near 280 nm where the latter system shows negative and the former positive ellipticities. So far, it is not clear what the related structural differences of the complexes are.

4.3. *With Complementary DNA.* The α-D-bicyclooligonucleotides α-bcd(A_{10}) and α-bcd(T_{10}) also form stable duplexes with their natural β-D-complement as can be seen from the corresponding melting curves (*Fig. 7, a*; T_m values in *Table 3*). To check the possibility of triplex formation, we recorded UV/mixing curves in the two pairing systems under discussion (*Fig. 7, b*). Under high salt concentration conditions (1M NaCl), in neither of the two systems triplex formation can be observed. The intersection points of both curves are in the range of 50 mol-% β-d(T_{10}) or α-bcd(T_{10}), respectively, indicating only duplex formation. CD Spectra of the two duplexes (*Fig. 7, c* and *d*) at various temperatures reflect the structural transitions related to duplex melting and furthermore indicate a substantial degree of structural similarity of the two duplexes. In the non-denatured state, characteristic strong negative *Cotton* effects between 240 and 250 nm and two positive maxima at 263 and 282 nm, respectively, are observed. The two duplexes mainly differ in the relative amplitude of the signal between 255 and 270 nm. In general, the spectra of both duplexes are surprisingly similar to that of the purely natural duplex β-d(A_{10})·β-d(T_{10}) but quite different from that of β-d(A_8)·α-d(T_8) [22]. Especially in the range above 260 nm, the CD signals of the duplex β-d(A_8)·α-d(T_8) show opposite sign compared to those of β-d(A_{10})·α-bcd(T_{10}). Whether the structural differ-

Table 3. T_m *Values, Thermodynamic Data, and Salt Sensitivity of Duplex Formation.* Conditions as indicated in *Figs. 6–10.*

Duplex	ΔH [kcal/mol]	ΔS [cal/mol K]	ΔG(25°C) [kcal/mol]	T_m [°C]	$\delta T_m/\delta \ln$ [NaCl]	Δn
α-bcd(A_{10})·α-bcd(T_{10})	–41.4	–114.7	–7.2	22.0	9.6	4.9
α-bcd(A_{10})·β-bcd(T_{10})	–60.5	–177.0	–7.7	25.2	6.8	4.7
β-bcd(A_{10})·α-bcd(T_{10})	–48.8	–121.5	–12.6	58.5	11.0	4.9
β-d(A_{10})·α-bcd(T_{10})	–45.0	–124.1	–8.0	26.7	7.8	3.9
α-bcd(A_{10})·β-d(T_{10})	–64.6	–185.2	–9.4	32.9	5.4	3.7

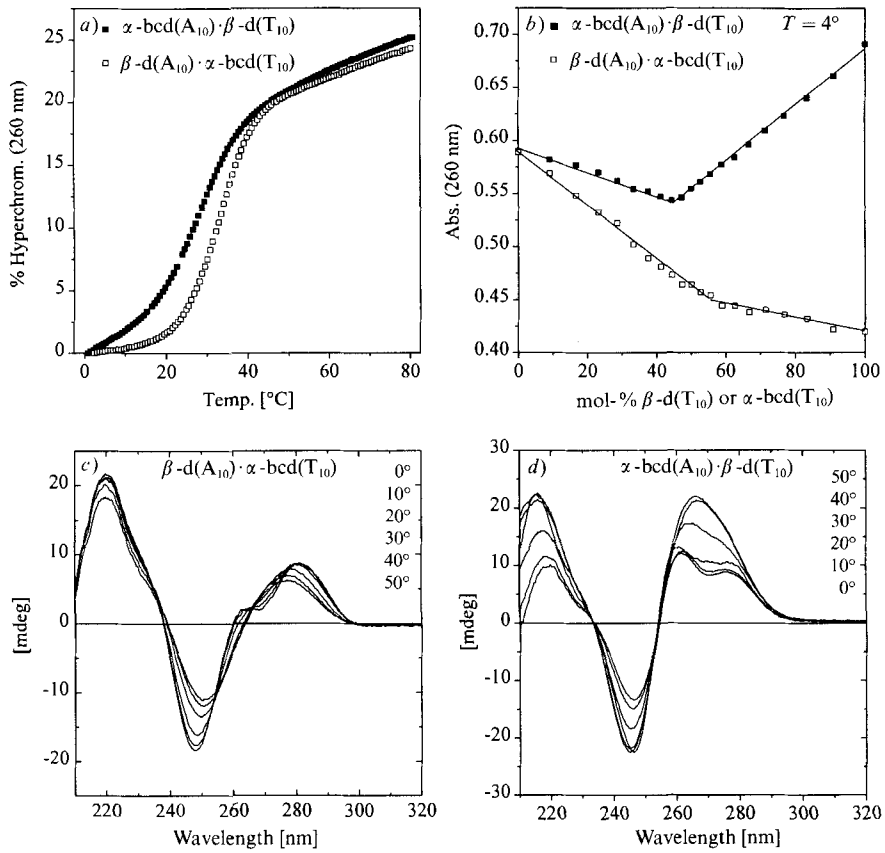

Fig. 7. a) *UV/Melting curves*, b) *UV/mixing curves, and* c) d) *CD spectra of α-bcd(A$_{10}$)·β-d(T$_{10}$) and β-d(A$_{10}$)·α-bcd(T$_{10}$) in 10 mM NaH_2PO_4, 1 M NaCl, pH 7.0 (c = 5.7 μM)*

ences arise from different polarity of the strand alignment, from non-*Watson-Crick* base pairing, or simply from differences in the helical parameters within the two duplexes, however, remains subject of speculation.

We calculated thermodynamic data for duplex formation (*Table 3*) from $1/T_m$ *vs.* ln c plots [23] (c = [NaCl]) and found remarkable differences in ΔH and ΔS values. Exchanging the purine strand by α-bcd(A$_{10}$) in the natural duplex β-d(A$_{10}$)·β-d(T$_{10}$) has almost no effect on the thermodynamic data ΔH, ΔS, and ΔG, whereas exchanging the pyrimidine strand by α-bcd(T$_{10}$) is accompanied by a compensating change in pairing enthalpy and entropy, leading to a duplex with slightly reduced thermodynamic stability (ΔG) with respect to the parent natural system.

Oligonucleotide duplex stability is strongly dependent on the amount of salt present in the medium. Increasing salt concentration stabilizes duplex formation because of the following two reasons: *i*) shielding of the negative charges by counter ions and

ii) differential counter-ion uptake upon duplexation. The latter effect, mainly entropic in nature, is dominant at monovalent salt concentrations below 1M. From plots of T_m *vs.* ln[NaCl] (*Fig. 8*), the sensitivity of duplex formation to the concentration of NaCl (10 mM – 0.6M) in the systems mentioned can be evaluated.

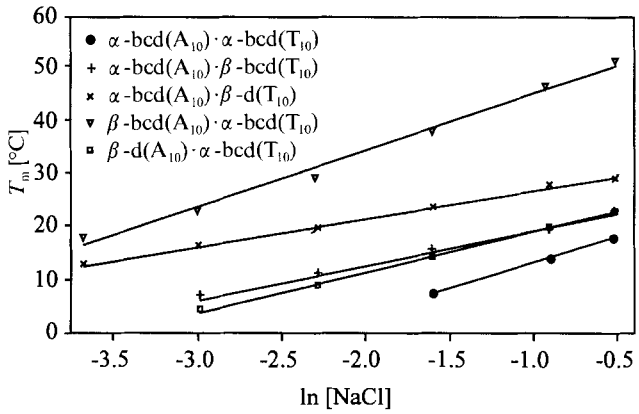

Fig. 8. *Dependence of* T_m *from [NaCl] for the duplexes indicated* (10 mM NaH_2PO_4, pH 7.0, c = 4.3–5.6 μM)

In all cases, as expected, a linear relationship between T_m and ln[NaCl] is observed. From the data for duplex-formation enthalpy (ΔH) and the values $\delta T_m/\delta$ln[NaCl] (*Table 3*), the number of cations that are taken up from the medium upon duplex formation (Δn) according to the polyelectrolyte theory (*Eqn. 1*) [24] [25] are calculated (*Table 3*).

$$\Delta n = -\frac{\delta T_m}{\delta \ln[\mathrm{NaCl}]} \cdot \frac{2\Delta H}{RT_m^2} \tag{1}$$

The $\delta T_m/\delta$ln[NaCl] values for the two duplexes are slightly different being larger in β-d(A_{10})·α-bcd(T_{10}) than in α-bcd(A_{10})·β-d(T_{10}). This relative difference only reflects the discrepancy between the pairing enthalpies in the two systems, since the extent of counter-ion uptake for both systems is almost the same and in the range of the corresponding purely natural duplex β-d(A_{10})·β-d(T_{10}) [15].

We identified the preferred orientation of the nucleotide chains in α-bicyclo-DNA/β-DNA duplexes by recording melting curves of mixtures between the unsymmetrical decamer sequence α-bcd(T-T-A-A-A-T-T-A-T-A) and its parallel (d-(A-A-T-T-T-A-A-T-A-T)) as well as its antiparallel (d-(T-A-T-A-A-T-T-T-A-A)) oriented natural β-D-complement (*Fig. 9a*). Only in the case of parallel strand alignment, cooperative melting is observed. As in the case of α-DNA, α-bicyclo-DNA prefers parallel chain orientation, with *Watson-Crick* base pairing in its duplexes with natural β-DNA.

4.4. *With Complementary* α- *and* β-*Bicyclo-DNA*. UV/Melting curves of the three duplexes α-bcd(A_{10})·α-bcd(T_{10}), α-bcd(A_{10})·β-bcd(T_{10}), and β-bcd(A_{10})·α-bcd(T_{10}) (*Fig. 10, a*) provide a quite heterogeneous picture of duplex stability in each system,

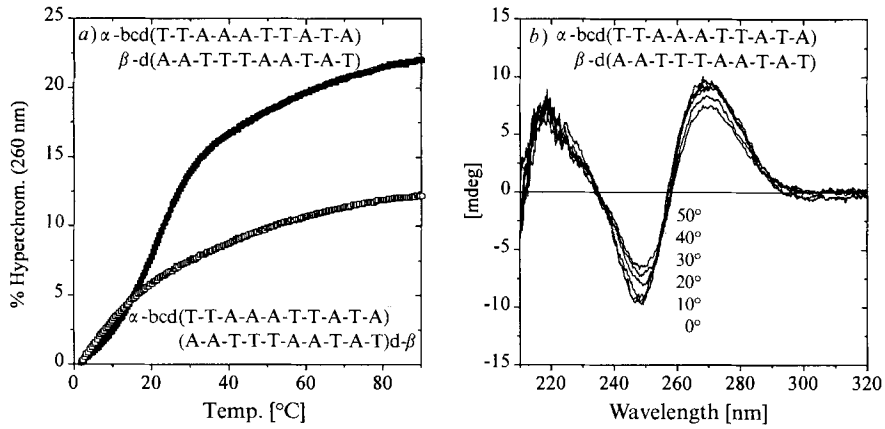

Fig. 9. a) *UV/Melting curves of mixtures of the sequence α-bcd(T-T-A-A-A-T-T-A-T-A) with parallel and antiparallel natural-DNA complement;* b) *CD spectra of the parallel oriented duplex* (10 mM NaH_2PO_4, 1M NaCl, pH 7.0, c = 5.2–5.7 μM)

characterizing the last duplex as exceptionally stable compared to the others. From inspection of the thermodynamic data in *Table 3*, it becomes evident that the counter-ion uptake upon duplexation is similar within the purely bicyclic duplexes (Δn = 4.7–4.9) but is distinctly larger than in the mixed natural/bicyclic duplexes (Δn = 3.7–3.9). This results in a higher sensitivity of the T_m from the salt concentration and can be responsible for a considerable loss of binding energy at low salt concentration in the medium. The duplex β-bcd(A_{10})·α-bcd(T_{10}) is comparable in stability to that of β-bcd(A_{10})·β-bcd(T_{10}), which under the same conditions shows a T_m value of 55° [15]. While the CD spectra of the two duplexes containing α-bcd(A_{10}) (*Fig. 10, b* and *c*) are similar and essentially reflect again the characteristics of that of natural β-d(A_{10})·β-d(T_{10}), that of the duplex β-bcd(A_{10})·α-bcd(T_{10}) differs significantly, showing negative ellipticities below 215 nm and around 280 nm (*Fig. 10, d*). Most interestingly, this CD spectrum almost matches that of β-bcd(A_{10})·β-bcd(T_{10}) [15] and resembles that of poly(A)·α-d(T_8) [22].

5. Nuclease Stability. – We showed previously that β-D-oligo(bicyclonucleotides) are considerably more stable against nuclease S1 (S1) and calf-spleen phosphodiesterase (CSP; by factors of 10^2 and 10^3, resp.) and modestly more stable (by a factor of 3–6) against snake-venom phosphodiesterase (SVP) than natural β-D-oligonucleotides [3]. In contrast, a change of configuration at the anomeric center alone, as in the case of α-DNA, dramatically increases the stability against SVP [10]. We tested the sequences α-bcd(A_{10}),α-bcd(T_{10}), and α-bcd(T_{20}) for resistance against phosphodiester hydrolysis catalyzed by SVP. Half-lifes ($t_{1/2}$) are summarized in *Table 4*. α-Bicyclo-DNA displays more than 100-fold higher stability (with respect to natural β-DNA) against this very potent enzyme. To compare the enzymatic resistance of α-bicyclo-DNA with that of α-DNA, we synthesized the sequence α-d(T_{20}) and compared its enzymatic stability with that of α-bcd(T_{20}). We were surprised to find that the enzyme SVP hydrolyzes both

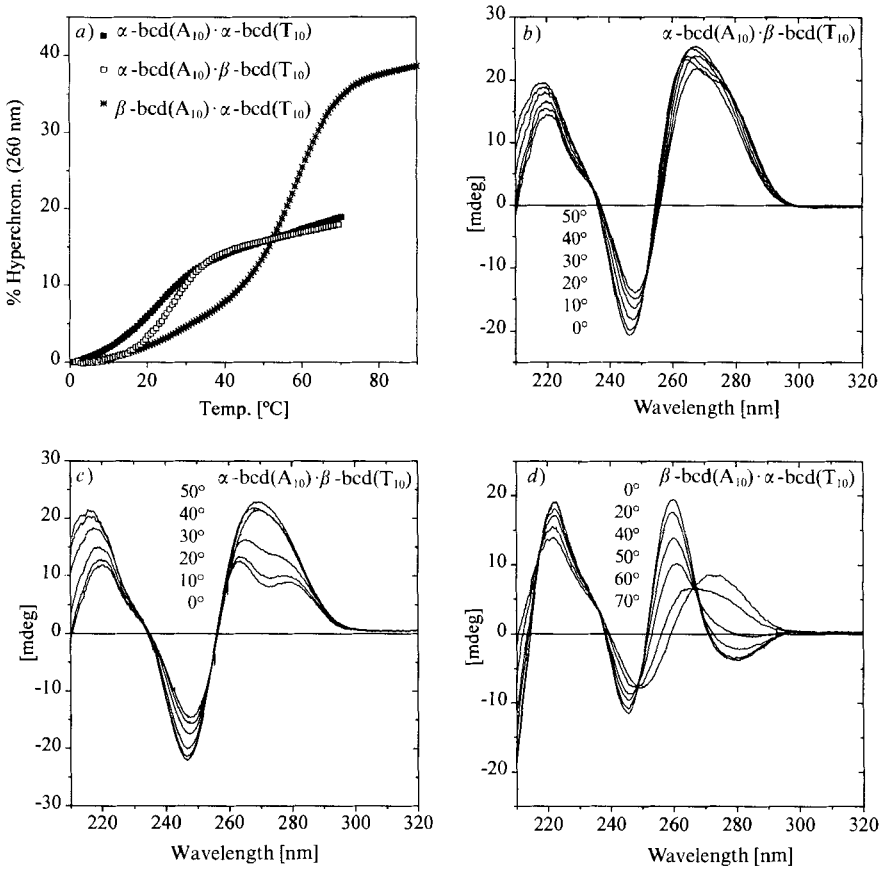

Fig. 10. a) *UV/Melting curves and* b) c) d) *CD spectra of the bicyclo-DNA duplexes indicated* (10 mM NaH_2PO_4, 1M NaCl, pH 7.0, c = 5.2–6.7 μM)

sequences with almost identical rate. Essentially, only the change of configuration at the anomeric center and not the structural differences within the carbohydrate residue is responsible for the higher enzymatic stability.

6. Conclusions. – The experiments presented here document the ability of α-bicyclo-DNA containing the bases adenine and thymine to form complexes with complementary natural RNA and DNA. These hybrid duplexes (or triplexes) are generally of equal or slightly diminished thermodynamic stability compared to the corresponding β-

Table 4. *Half-lifes of α-D-Oligonucleotides against Snake-Venom Phosphodiesterase*

Sequence	α-bcd(A_{10})	α-bcd(T_{10})	α-bcd(T_{20})	α-d(T_{20})
$t_{1/2}$ [min] (conc. [μM])[a])	156 (16.1)	510 (16.7)	782 (8.6)	806 (8.7)

[a]) Conditions, see *Exper. Part.*

DNA, RNA or β-DNA, β-DNA complexes. In general, the biophysical and biochemical data available on α-bicyclo-DNA in complexes with natural complementary DNA and RNA compare well with those of α-DNA. In evaluating α-bicyclo-DNA as a suitable candidate for antisense or antigene applications, clearly more data, as *e.g.* the potential to induce RNase H activity and bioavailability, would be necessary.

An interesting difference in structure and stability arises in purely bicyclic bcd(A_{10})·bcd(T_{10}) duplexes depending on the anomeric configuration of the nucleosides in the purine strand. This becomes evident when one compares UV/melting curves and CD spectra of duplexes containing α-bcd(A_{10}) with those containing β-bcd(A_{10}). The elucidation of the base-pairing modes in these duplexes is subject of further investigations.

As a structural consequence of the oxabicyclo[3.3.0]octane system, the torsion angle γ (*ca.* 150°) in the bicyclonucleosides is preorganized in a geometry that differs by *ca.* 90–100° from that generally observed in duplexes of α- and β-DNA (*ca.* 50–60°). It is important to realize that despite of this change, complementary duplex formation with natural DNA and RNA is still possible in both the α- and β-bicyclo-DNA series. A detailed structural analysis of the backbone torsion angles on the oligomeric level by 2D-NMR methods is under way in the β-bicyclo series and will shed light on the compensating structural changes of internucleoside (phosphoester bond) torsion angles accompanying the shift of γ.

This work was supported in part by the *Swiss National Science Foundation*, by *Ciba-Geigy AG*, Basel, and by the *Stiftung zur Förderung der wissenschaftlichen Forschung an der Universität Bern.*

Experimental Part

General. For reagents, solvents, and anal. instrumentation used in the synthesis and characterization of monomer building blocks, see [13]. Phosphodiesterase from *Crotalus durissus* (EC 3.1.15.1): *Böhringer*, Mannheim. HPLC: *Pharmacia-LKB-2249* gradient pump attached to an *ABI-Kratos-Spectroflow-757* UV/VIS detector and a *Tarkan W + W* recorder *600* or *HP-3396A*-integrator. Capillary gel electrophoresis (CE): *Waters Quanta 4000* connected to a *Waters 746* data module; capillary, *μPage* (5%T, 5%C) fused silica capillary (75 cm × 75 μm, *J&W Scientific*); buffer, 100 mM *Tris*·borate, 7M urea, pH 8.3; voltage, 12.5 kV. Extinction coefficients of oligonucleotides were experimentally determined by relating the UV absorption of an aliquot of the oligonucleotide soln. (180 mM NaCl, 12 mM *Tris*·HCl, pH 7.0, 25°) at 260 nm with that of the free monomeric units after complete digestion of the aliquot with snake-venom phosphodiesterase/alkaline phosphatase (HPLC control) according to the formula $\varepsilon(\text{oligo}) = (D_{\text{start}}/D_{\text{end}}) \cdot \sum_{i=1}^{n} \varepsilon_i(\text{mono})$ where the ε(mono)'s refer to the extinction coefficients of the monomers at 260 nm (25° in H_2O). Matrix-assisted laser-desorption-ionization time-of-flight mass spectrometry (MALDI-TOF-MS) of oligonucleotides was performed as described [26]. UV/Melting curves: *Varian-Cary-3E* UV/VIS spectrometer equipped with a temperature-controller unit and connected to a *Compaq-ProLinea-3/25-zs* personal computer. Temperature gradients of 0.5°/min were applied, and data points were collected in intervals of *ca.* 0.3°. At temps. below 20°, the cell compartment was flushed with N_2 to avoid condensation of H_2O on the UV cells. %Hyperchrom. (wavelength) = $100 \cdot [(D(T) - D_o)/D_o]$, with $D(T)$ = absorption at temp. T and D_o = lowest absorption in the temp. interval. The transition temperature T_m was determined as described [23]. CD Spectra: *Jasco-J-500A* spectropolarimeter with *IF-500-II* interface connected to a *PC/AT* personal computer. The cell was thermostated by a *Julabo-F20* circulating bath. Temp. were determined directly in the sample soln.

(3′S,5′R)-1-{2′-Deoxy-5′-O-[(4,4′-dimethoxytriphenyl)methyl]-3′,5′-ethano-α-D-ribofuranosyl}thymine (**8**). To a stirred soln. of dry α-D-bicyclothymidine **1** [13] (239 mg, 0.894 mmol) in pyridine (2 ml) was added $[(MeO)_2Tr]CF_3SO_3$ (404 mg, 0.894 mmol, 1.0 equiv.) [13] under Ar at r.t. In intervals of 30 min, three further portions of $[(MeO)_2Tr]CF_3SO_3$ (1.0, 0.5, 0.5 equiv.) were added. After a total of 2 h, the mixture was diluted with CH_2Cl_2 (30 ml) and sat. $NaHCO_3$ soln. (30 ml), the aq. layer extracted with CH_2Cl_2 (2 × 30 ml), and the combined

org. phase dried ($MgSO_4$) and evaporated. The resulting yellow oil was purified by CC (silica gel, CH_2Cl_2/MeOH 50:1) and dried (h.v., 3 h, r.t.): 532 mg (corr. 94%) of **8** containing 10% of pyridine (^{1}H-NMR). White foam. TLC (CH_2Cl_2/MeOH): R_f 0.60. IR ($CHCl_3$): 3395*m*, 3006*m*, 2959*m*, 2838*w*, 1687*s*, 1608*m*, 1582*w*, 1509*s*, 1464*m*, 1361*m*, 1301*m*, 1251*s*, 1154*m*, 1117*m*, 1074*m*, 1036*m*, 1002*m*, 910*w*, 836*m*. ^{1}H-NMR (400 MHz, $CDCl_3$): 1.35–1.47, 1.75–1.84 (2*m*, 2 H–C(6′), 2 H–C(7′)); 1.92 (*d*, *J* = 1.1, Me–C(5)); 2.49 (*dd*, *J* = 3.9, 14.8, H–C(2′)); 2.53 (*dd*, *J* = 7.0, 14.8, H–C(2′)); 3.45 (*s*, OH–C(3′)); 3.69 (*d*, *J* = 5.5, H–C(4′)); 3.78 (*s*, MeO); 3.88–3.96 (*m*, H–C(5′)); 5.95 (*dd*, *J* = 3.8, 6.9, H–C(1′)); 6.80–6.84 (*m*, 4 arom. H); 7.12 (*d*, *J* = 1.2, H–C(6)); 7.19–7.23 (*m*, 1 arom. H); 7.26–7.30 (*m*, 2 arom. H); 7.39–7.43 (*m*, 4 arom. H); 7.50–7.53 (*m*, 2 arom. H); 9.02 (br. *s*, NH). ^{13}C-NMR (100 MHz, $CDCl_3$): 12.4 (*q*, *Me*–C(5)); 29.9, 35.4 (2*t*, C(6′), C(7′)); 47.8 (*t*, C(2′)); 55.2 (*q*, MeO); 74.2 (*d*, C(5′)); 85.9, 87.0 (2*s*, C(3′), Ar_2CPh); 90.8, 91.3 (2*d*, C(1′), C(4′)); 110.4 (*s*, C(5)); 113.1, 126.8, 127.9, 128.3, 130.2 (5*d*, arom. C); 136.8, 136.9, 145.6, 158.6 (4*s*, arom. C); 138.3 (*d*, C(6)); 150.5 (*s*, C(2)); 164.0 (*s*, C(4)). FAB-MS (pos.): 571 (2.2, $[M + 1]^+$), 570 (1.9, M^+), 304 (28), 303 (100).

*(3′S,5′R)-N^6-Benzoyl-9-{2′-deoxy-5′-O-[(4,4′-dimethoxytriphenyl)methyl]-3′,5′-ethano-α-*D*-ribofuranosyl}-adenine* (**9**). To a soln. of dry N^6-benzoyl-α-D-bicyclodeoxyadenosine **5** [13] (700 mg, 1.824 mmol) in pyridine (5 ml) were added $[(MeO)_2Tr]CF_3SO_3$ (1.185 g, 2.62 mmol, 1.4 equiv.) [15] under Ar. After 40 and 80 min stirring at r.t., additional 593 mg (1.31 mmol, 0.7 equiv.) of $[(MeO)_2Tr]CF_3SO_3$ were added. After a total of 2 h, the mixture was worked up as described for **8**. The yellow-brown foam was purified by CC (silica gel, CH_2Cl_2/MeOH 50:1) to give 1000 mg (79%) of **9**, after precipitation from 600 ml of Et_2O/pentane 2:1. Beige powder. TLC (CH_2Cl_2/MeOH 10:1): R_f 0.66. IR ($CHCl_3$): 3286*m* (br.), 3005*m*, 2838*w*, 1711*m*, 1613*s*, 1585*s*, 1509*s*, 1458*s*, 1418*w*, 1332*m*, 1300*m*, 1248*s*, 1190*m*, 1069*s*, 1035*m*, 1004*w*, 900*w*, 830*m*, 647*w*, 625*w*. ^{1}H-NMR (400 MHz, $CDCl_3$): 1.56–1.75, 1.82–1.93 (2*m*, 2 H–C(6′), 2 H–C(7′)); 2.74 (*dd*, *J* = 8.6, 15.4, 1 H–C(2′)); 2.95 (*d*, *J* = 15.5, 1 H–C(2′)); 3.09 (*d*, *J* = 4.7, H–C(4′)); 3.90–3.95 (*m*, H–C(5′)); 6.25 (*d*, *J* = 7.3, H–C(1′)); 6.63–6.68 (*m*, 2 arom. H); 7.07 (*t*, *J* = 7.3, 1 arom. H); 7.16–7.20 (*m*, 2 arom. H); 7.35 (*d*, *J* = 8.9, 4 arom. H); 7.45–7.47 (*m*, 2 arom. H); 7.64 (*t*, *J* = 7.3, 1 arom. H); 8.05, 8.73 (2*s*, H–C(2), H–C(8)); 7.06 (*d*, *J* = 8.7, 2 arom. H); 9.22 (*s*, NH). ^{13}C-NMR (100 MHz, $CDCl_3$): 29.2, 36.1 (2*t*, C(6′), C(7′)); 47.9 (*t*, C(2′)); 55.2 (*q*, MeO); 74.7 (*d*, C(5′)); 85.2, 87.2 (2*s*, C(3′), Ar_2CPh); 87.0, 89.5 (2*d*, C(1′), C(4′)); 112.91, 112.93, 126.6, 127.8, 127.9, 128.0, 129.0, 129.2, 130.06, 130.13, 133.0 (11*d*, arom. C); 123.8 (*s*, C(5)); 133.6, 136.4, 136.8, 145.5, 158.47, 158.51 (6*s*, arom. C); 144.3 (*d*, C(8)); 150.0, 150.2 (2*s*, C(4), C(6)); 151.6 (*d*, C(2)); 164.4 (*s*, CO). FAB-MS (pos.): 685 (2.3, $[M + 1]^+$), 684 (5.1, M^+), 304 (28), 303 (100).

*(3′S,5′R)-1-{3′-O-[(Allyloxy)(diisopropylamino)phosphino]-2′-deoxy-5′-O-[(4,4′-dimethoxytriphenyl)-methyl]-3′,5′-ethano-α-*D*-ribofuranosyl}thymine* (**10**). To a stirred soln. of **8** (384 mg, 0.673 mmol) in THF (2 ml) were added $(i\text{-}Pr)_2EtN$ (460 µl, 2.69 mmol, 4.0 equiv.) and (allyloxy)chloro(diisopropylamino)phosphine (300 µl, 1.35 mmol, 2.0 equiv.) under Ar at r.t. After 2 h, the resulting mixture was diluted with AcOEt (30 ml) and sat. $NaHCO_3$ soln. (30 ml), the aq. phase extracted with AcOEt (2 × 30 ml), and the combined org. phase dried ($MgSO_4$) and evaporated. Purification of the crude product by CC (silica gel, hexane/AcOEt 1:1) provided **10** (405 mg, 79%; *ca.* 1:1 mixture of diastereoisomers by ^{1}H-NMR). White foam. TLC (hexane/AcOEt 1:2): R_f 0.73. IR ($CHCl_3$): 3398*m*, 3006*m*, 2968*m*, 2873*w*, 2838*w*, 1683*s*, 1608*m*, 1509*s*, 1464*m*, 1397*m*, 1364*m*, 1251*s*, 1156*m*, 1120*m*, 1080*m*, 1034*s*, 976*m*, 932*m*, 877*w*, 838*m*, 817*m*, 641*w*. ^{1}H-NMR (400 MHz, $CDCl_3$): 1.02, 1.06, 1.10 (3*d*, *J* = 6.8, 2 Me_2CH); 1.37–1.64, 1.68–1.88, 1.94–2.10 (3*m*, 2 H–C(6′), 2 H–C(7′)); 1.94 (*s*, Me–C(5)); 2.41 (*dd*, *J* = 7.0, 14.7, 0.5 H, H–C(2′)); 2.52 (*dd*, *J* = 6.8, 14.7, 0.5 H, H–C(2′)); 2.59 (*dd*, *J* = 2.0, 14.8, 0.5 H, H–C(2′)); 2.70 (*dd*, *J* = 3.0, 14.6, 0.5 H, H–C(2′)); 3.45, 3.47 (2 *sept.*, *J* = 6.8, 2 Me_2CH); 3.62 (*d*, *J* = 5.7, 0.5 H, H–C(4′)); 3.794, 3.798 (2*s*, MeO); 3.84–3.97, 3.98–4.08 (2*m*, 3.5 H, H–C(4′), H–C(5′), CH_2=$CHCH_2O$); 5.07–5.11, 5.14–5.24 (2*m*, CH_2=$CHCH_2O$); 5.82, 5.85 (2*m*, *J* = 5.4, CH_2=$CHCH_2O$); 6.26–6.30 (*m*, H–C(1′)); 6.83–6.86 (*m*, 4 arom. H); 7.15 (*d*, *J* = 1.2, 0.5 H, H–C(6)); 7.21–7.25 (*m*, 1.5 H, H–C(6), arom. H); 7.28–7.32 (*m*, 2 arom. H); 7.42–7.46 (*m*, 4 arom. H); 7.53–7.55 (*m*, 2 arom. H); 8.39 (br. *s*, NH). ^{13}C-NMR (100 MHz, $CDCl_3$): 12.3, 12.4 (2*q*, *Me*–C(5)); 24.1, 24.16, 24.19, 24.27, 24.32 (5*q*, Me_2CH); 30.4, 30.6 (2*t*, C(6′)); 33.45, 33.75 (2*td*, *J*(C,P) = 11.6, C(7′)); 42.95, 43.075 (2*dd*, Me_2CH); 46.02 (*td*, *J*(C,P) = 5.9, C(2′)); 47.64 (*td*, *J*(C,P) = 6.6, C(2′)); 55.2 (*q*, MeO); 63.65 (*td*, *J*(C,P) = 7.3, CH_2=$CHCH_2O$); 63.85 (*td*, *J*(C,P) = 8.2, CH_2=$CHCH_2O$); 73.2, 73.3 (2*d*, C(5′)); 86.9 (*s*, Ar_2CPh); 88.3, 88.5 (2*d*, C(1′)); 89.34 (*sd*, *J*(C,P) = 10.0, C(3′)); 89.52 (*sd*, *J*(C,P) = 5.7, C(4′)); 89.56 (*sd*, *J*(C,P) = 9.1, C(3′)); 90.21 (*sd*, *J*(C,P) = 5.3, C(4′)); 109.4, 109.7 (2*s*, C(5)); 113.0, 126.8, 127.8, 127.9, 128.1, 128.4, 130.20, 130.22, 130.24 (9*d*, arom. C); 115.9, 116.0 (2*t*, CH_2=$CHCH_2O$); 135.23, 135.34 (2*dd*, *J*(C,P) = 7.7, CH_2=$CHCH_2O$); 136.4, 136.6 (2*d*, C(6)); 136.80, 136.84, 136.9, 145.49, 145.50, 158.50, 158.53 (7*s*, arom. C); 150.09, 150.12 (2*s*, C(2)); 163.9 (*s*, C(4)). ^{31}P-NMR (162 MHz, $CDCl_3$): 142.1, 142.6. FAB-MS (pos.): 758 (2.4, $[M + 1]^+$), 304 (38), 303 (100).

*(3′S,5′R)-9-{3′-O-[(Allyloxy)(diisopropylamino)phosphino]-2′-deoxy-5′-O-[(4,4′-dimethoxytriphenyl)-methyl]-3′,5′-ethano-α-*D*-ribofuranosyl}-N^6-benzoyladenine* (**11**). To a stirred soln. of **9** (685 mg, 1.00 mmol) in THF (10 ml) were added $(i\text{-}Pr)_2EtN$ (820 µl, 4.8 mmol, 4.8 equiv.) and (allyloxy)chloro(diisopropyl-

amino)phosphine (540 µl, 2.4 mmol, 2.4 equiv.) under Ar at r.t. Additional two portions of $(i\text{-Pr})_2EtN$ (820 µl, 4.8 mmol, 4.8 equiv.) and (allyloxy)chloro(diisopropylamino)phosphine (540 ml, 2.4 mmol, 2.4 equiv.) were added in intervals of 90 min. After a total reaction time of 4.5 h, the resulting mixture was worked up as described for **10** (AcOEt (50 ml), sat. $NaHCO_3$ soln. (50 ml), AcOEt (2 × 50 ml)). CC (silica gel, hexane/AcOEt 1:2), followed by repetitive precipitation (4×) from hexane (200 ml, –60°) provided **11** (703 mg, 81%; *ca.* 1:1 mixture of diastereoisomers (^{1}H-NMR)). White powder. TLC (hexane/AcOEt 1:2): R_f 0.60. IR ($CHCl_3$): 3410*w*, 3003*m*, 2969*m*, 2839*w*, 1707*m*, 1611*s-m*, 1584*m*, 1509*s*, 1455*s*, 1396*m*, 1364*m*, 1298*m*, 1252*s*, 1157*m*, 1123*m*, 1087*m*, 1068*m*, 1034*m*, 977*m*, 934*m*, 830*m*, 641*w*. ^{1}H-NMR (400 MHz, $CDCl_3$): 0.85, 0.96, 1.04 (3*d*, J = 6.8, 2 Me_2CH); 1.56–1.63, 1.67–1.71, 1.74–2.03 (3*m*, 2 H–C(6′), 2 H–C(7′)); 2.52, 2.62 (2*dd*, J = 6.9, J = 14.6, 1 H–C(2′)); 3.11–3.27 (*m*, 1 H–C(2′)); 3.30–3.42 (*m*, 2 Me_2CH); 3.50 (*d*, J = 4.8, 0.5 H, H–C(4′)); 3.778, 3.781, 3.790, 3.792 (4*s*, 2 MeO); 3.80–4.00 (*m*, 3.5 H, H–C(4′), H–C(5′), CH_2=CHCH_2O); 4.99–5.19 (*m*, CH_2=CHCH_2O); 5.71, 5.80 (2*ddd*, J = 5.3, 10.5, 17.1, CH_2=CH_2CH_2O); 6.55–6.58 (*m*, H–C(1′)); 6.77–6.85 (*m*, 4 arom. H); 7.19–7.29 (*m*, 3 arom. H); 7.41–7.45 (*m*, 4 arom. H); 7.52, 7.56 (*m*, 4 arom. H); 7.60–7.64 (*m*, 1 arom. H); 8.03 (*d*, J = 7.3, 2 arom. H); 8.18, 8.20, 8.816, 8.825 (4*s*, H–C(2), H–C(8)); 9.05 (br. *s*, NH). ^{13}C-NMR (100 MHz, $CDCl_3$); 24.0, 24.1, 24.2, 24.27, 24.29, 24.31, 24.37 (7*q*, Me_2CH); 30.1, 30.2 (2*t*, C(6′)); 34.1 (*td*, J(C,P) = 11.5, C(7′)); 34.5 (*td*, J(C,P) = 13.8, C(7′)); 42.9, 43.1 (2*dd*, J(C,P) = 12.6, Me_2CH); 43.0, 43.1 (2*d*, J(C,P) = 12.6, Me_2CH); 47.0, 47.1, 48.0 (3*t*, C(2′)); 55.22, 55.24 (2*q*, MeO); 63.5, 63.6 (2*t*, J(C,P) = 17.1, CH_2=CHCH_2O); 63.7, 63.9 (2*t*, J(C,P) = 17.7, CH_2=CHCH_2O); 73.6, 73.7 (2*d*, C(5′)); 86.5 (*d*, C(1′)); 87.0 (*s*, Ar_2CPh); 89.09 (*dd*, J(C,P) = 5.5, C(4′)); 89.24 (*dd*, J(C,P) = 6.0, C(4′)); 89.45 (*sd*, J(C,P) = 9.1, C(3′)); 89.60 (*sd*, J(C,P) = 9.2, C(3′)); 113.09, 113.13, 126.9, 127.8, 128.4, 128.9, 130.2, 132.7 (8*d*, arom. C); 115.7, 115.8 (2*t*, CH_2=CHCH$_2$O); 123.1 (*s*, C(5)); 134.0, 136.78, 136.81, 136.9, 135.4, 145.5, 158.6 (7*s*, arom. C); 135.15 (*dd*, J(C,P) = 7.7, CH_2=CHCH$_2$O); 135.35 (*dd*, J(C,P) = 7.5, CH_2=CHCH$_2$O); 141.8, 141.9 (2*d*, C(8)); 149.16, 149.21 (2*s*, C(4)); 151.3, 151.5 (2*s*, C(6)); 152.5 (*d*, C(2)); 164.5 (*s*, CO). ^{31}P-NMR (162 MHz, $CDCl_3$): 142.2, 142.4. FAB-MS (pos.): 871 (1.8, M^+), 304 (32), 303 (100).

*(3′*S*,5′*R*)-1-{2′-Deoxy-5′-O-[(4,4′-dimethoxytriphenyl)methyl]-3′,5′-ethano-3′-O-[4-(4-nitrophenyloxy)-succinyl]-α-*D*-ribofuranosyl}thymine* (**12**). A mixture of **8** (150 mg, 0.263 mmol), succinic anhydride (263 mg, 2.63 mmol, 10 equiv.), and 4-(dimethylamino)pyridine (160 mg, 1.32 mmol, 5 equiv.) in pyridine (1 ml) was stirred at r.t. After 67 h, the resulting dark soln. was diluted with sat. $NaHCO_3$ soln. (20 ml) and extracted with CH_2Cl_2 (3 × 20 ml). The combined org. phases were washed with 10% citric acid (20 ml), dried (Na_2SO_4), and evaporated. To the residual brownish foam (200 mg) in dioxane (1 ml) were added 4-nitrophenol (51 mg, 0.364 mmol, 1.4 equiv.) and dicyclohexylcarbodiimide (DCC; 163 mg, 0.781 mmol, 3 equiv.). The resulting soln. was stirred for 120 min at r.t., diluted with H_2O (200 µl), and filtered, the solid washed with AcOEt (10 ml), and the filtrate evaporated. CC of the crude residue (silica gel, hexane/AcOEt 1:3) gave **12** (176 mg, 85%). White foam. TLC (hexane/AcOEt 1:2): R_f 0.46. UV ($CHCl_3$): 269 (17600). IR ($CHCl_3$): 3380*w*, 2940*w*, 2920*w*, 1760*m*, 1735*m*, 1680*s*, 1605*m*, 1590*m*, 1500*m*, 1460*m*, 1295*s*, 1125*s*, 1080*m*, 1030*m*, 905*m*, 860*m*. ^{1}H-NMR (300 MHz, $CDCl_3$): 1.25–1.68, 2.05–2.12 (2*m*, H–C(6′), H–C(7′)); 1.86 (*s*, Me–C(5)); 2.42–2.49, 2.67–2.78 (2*m*, H–C(2′), OCCH_2CH_2CO); 3.71 (*s*, MeO); 3.79 (*d*, J = 5.5, H–C(4′)); 3.93–3.99 (*m*, H–C(5′)); 6.19 (*dd*, J = 4.2, 6.5, H–C(1′)); 6.77 (*d*, J = 8.9, 4 arom. H); 6.93 (*d*, J = 1.2, H–C(6)); 7.12–7.30 (*m*, 5 arom. H); 7.36 (*dd*, J = 3.0, 9.0, 4 arom. H); 7.44–7.46 (*m*, 2 arom. H); 8.18 (*d*, J = 9.1, 2 arom. H); 9.15 (br. *s*, NH). ^{13}C-NMR (75 MHz, $CDCl_3$): 12.7 (*q*, *Me*–C(5)); 29.1, 29.2 (2*t*, OCCH_2CH_2CO); 29.8, 32.7 (2*t*, C(6′), C(7′)); 45.6 (*t*, C(2′)); 55.4 (*q*, MeO); 73.4 (*d*, C(5′)); 87.2, 92.5 (2*s*, C(3′), Ar_2CPh); 88.03, 88.04 (2*d*, C(1′), C(4′)); 110.3 (*s*, C(5)); 113.3, 122.5, 125.4, 127.1, 128.0, 128.5, 130.3 (7*d*, arom. C); 135.4 (*d*, C(6)); 136.76, 136.83, 145.5, 155.3, 158.7 (5*s*, arom. C); 150.3 (*s*, C(2)); 164.0 (*s*, C(4)); 170.1, 171.1 (2*s*, CO). FAB-MS (pos.): 830 (2, $[M + 39]^+$), 814 (1, $[M + 23]^+$), 792 (0.5, $[M + 1]^+$), 303 (100).

*(3′*S*,5′*R*)-N^6-Benzoyl-9-{2′-deoxy-5′-O-[(4,4′-dimethoxytriphenyl)methyl]-3′,5′-ethano-3′-O-[4-(4-nitrophenyloxy)succinyl]-α-*D*-ribofuranosyl}adenine* (**13**). As described for **12**, with **9** (180 mg, 0.263 mmol), succinic anhydride (266 mg, 2.64 mmol, 10 equiv.), 4-(dimethylamino)pyridine (161 mg, 1.32 mmol, 5 equiv.), and pyridine (2 ml, 70 h). After workup with $NaHCO_3$ soln. (30 ml), CH_2Cl_2 (3 × 30 ml), and 2M citric acid (30 ml) and treatment of the brownish foam (204 mg) in dioxane (2 ml) with 4-nitrophenol (51 mg, 0.364 mmol, 1.4 equiv.) and DCC (165 mg, 0.781 mmol, 3 equiv.) for 80 min, the soln. was diluted with H_2O (250 µl), filtered, and washed with dioxane (10 ml) and AcOEt (10 ml) and the filtrate evaporated. CC of the crude residue (silica gel, AcOEt) gave **13** (197 mg, 84%). White foam. TLC (AcOEt): R_f 0.55. UV ($CHCl_3$): 278 (26600). IR ($CHCl_3$): 3410*w*, 2930*m*, 2915*w*, 2905*w*, 2840*w*, 1770*m*, 1740*m*, 1710*m*, 1610*s*, 1585*m*, 1510*s*, 1455*s*, 1425*m*, 1350*s*, 1300*m*, 1130*s*, 1090*m*, 1065*m*, 1060*m*, 1045*s*, 1030*s*, 925*s*, 910*m*, 625*m*. ^{1}H-NMR (300 MHz, $CDCl_3$): 1.50–1.70, 1.82–1.95, 2.11–2.19 (3*m*, 1 H–C(2′), 2 H–C(6′), 2 H–C(7′)); 2.25–2.32, 2.57–2.69 (2*m*, OCCH_2CH_2CO); 3.35 (*dd*, J = 1.9, 15.3, 1 H–C(2′)); 3.67 (*d*, J = 5.42, H–C(4′)); 3.70 (*s*, MeO); 3.94–4.04 (*m*, H–C(5′)); 6.41 (*dd*, J = 2.1, 6.4, H–C(1′)); 6.70–6.75 (*m*, 4 arom. H); 7.09–7.24 (*m*, 5 arom. H); 7.34 (*dd*, J = 2.3, 8.9, 4 arom. H); 7.42–7.50 (*m*, 4 arom. H); 7.52–7.55 (*m*, 1 arom. H); 7.87, 8.66 (2*s*, H–C(8), H–C(2)); 7.93 (*d*, J = 7.2, 2 arom. H); 8.12 (*d*, J = 9.1, 2 arom.

H); 9.00 (br. *s*, NH). ^{13}C-NMR (75 MHz, $CDCl_3$): 28.88, 28.93 (2*t*, $OCCH_2CH_2CO$); 30.1, 33.0 (2*t*, C(6'), C(7')); 45.0 (*t*, C(2')); 55.2 (*q*, MeO); 73.0 (*d*, C(5')); 86.9, 87.4 (2*d*, C(1'), C(4')); 87.1, 92.3 (2*s*, C(3'), Ar_2CPh); 113.1, 122.3, 125.2, 127.0, 127.8, 127.9, 128.3, 128.8, 130.1, 132.8, 141.3 (11*d*, arom. C); 123.4 (*s*, C(5)); 133.5, 136.5, 136.6, 136.7, 145.2, 145.3, 155.1, 158.6 (8*s*, arom. C); 141.5 (*d*, C(8)); 149.3 (*s*, C(4)); 151.4 (*s*, C(6)); 152.4 (*d*, C(2)); 164.5, 169.8, 170.9 (3*s*, CO). FAB-MS (pos.): 943 (4, $[M + 39]^+$), 927 (2, $[M + 23]^+$), 905 (5.0, $[M + 1]^+$), 303 (100).

Nucleoside-Modified Solid Support. Nucleoside-modified solid support was prepared from **12** and **13** and long-chain-alkylamine controlled-pore glass (LCAA-CPG) as described in [15]. In this way, 690 mg of α-bcdA- and 210 mg of α-bcdT-modified support (both with a loading capacity of 33 μmol/g) were obtained.

α-D-Oligo(bicyclodeoxyribonucleotides). Synthesis: Oligonucleotide synthesis was performed on a *Pharmacia-Gene-Assembler-Special* synthesizer connected to a *Compaq-Pro-Linea-3/25-zs* personal computer. All syntheses were performed using a modified 1.3-μmol cycle that met the reaction conditions given in *Scheme 2*. Solvents and solns. were made up according to the manufacturers protocol. The phosphoramidite (0.1M in MeCN) and 1*H*-tetrazole (0.5M in MeCN) solns. were equal in conc. to those used for the synthesis of natural oligodeoxynucleotides. Average coupling yields monitored by on-line trityl assay were generally in the range of 95–98%. All syntheses were run in the trityl-off mode.

Deprotection and Purification: Removal of the allyl protecting groups was performed in adapting the method of *Hayakawa et al.* [19]: The support was suspended in THF (2 ml) containing HCOOH (90 μl, and $BuNH_2$ (240 μl). Per allyl group, 1.5 equiv. of tris(dibenzylidenacetone)dipalladium(0) and 25 equiv. of PPh_3 were added, and the biphasic mixture was kept for 60–100 min at 55° by occasional shaking. The solid support was then filtered off, washed with THF (5 ml) and Me_2CO (5 ml), subsequently suspended in 0.1M aq. sodium diethyldithiocarbamate (4 ml, 15 min), and washed with H_2O (5 ml), Me_2CO (5 ml), and H_2O (5 ml). The diethyldithiocarbamate treatment was repeated once. Removal of the base-protecting groups (where present) and detachment from the solid support was then effected in conc. NH_3 soln. (3 ml) at 55° for 5–7 h. The crude oligomers where purified by HPLC to homogeneity using *DEAE* and reversed-phase chromatography systems, desalted over Sep-Pak (*Waters*), and stored as stock solns. in H_2O at −20°. *Table 5* contains synthetic and anal. data of the α-D-oligo(bicyclonucleotides) described here. All natural DNA sequences used in this study were prepared according to standard CED- or PAC-phosphoramidite chemistry and purified by HPLC.

Table 5. *Synthesis and Analytical Data of α-D-Oligo(bicyclodeoxynucleotides)*

Sequence (1.3 μmol)	HPLC	Isolated yield *OD* (260 nm) [%]	MALDI-TOF-MS $[M - H]^-$	
			m/z (calc.)	*m/z* (found)
α-bcd(T_{10})	*DEAE*[a]): 25–42% *B* in 35 min; t_R 19.5 min; reversed-phase[d]): 5–35% *B* in 30 min; t_R 16.5 min	30.3 (26)	3240.4	3240.9
α-bcd(A_{10})	*DEAE*[a]): 25–50% *B* in 35 min; t_R 26 min; reversed-phase[c]): 10–25% *B* in 30 min; t_R 16.5 min	39.1 (28)	3330.5	3331.9
α-bcd(T_{20})	*DEAE*[b]): 50–80% *B* in 30 min; t_R 24 min; reversed-phase[d]): 9–19% *B* in 30 min; t_R 21 min	55.0 (24)	6542.7	6545.0
α-bcd(T-T-A-A-A-T-T-A-T-A)	*DEAE*[b]): 25–50% *B* in 30 min; t_R 21 min; reversed-phase[c]): 5–30% *B* in 30 min; t_R 20 min	18.4 (18)	3284.4	3282.4

[a]) *Nucleogen DEAE 60-7*, 125 × 4.0 mm (*Macherey & Nagel*); *A* = 20 mM KH_2PO_4 in H_2O/MeCN 4:1, pH 6.0; *B* = *A* + 1M KCl; flow 1 ml/min; detection 260 nm.

[b]) *Nucleogen DEAE 60-7*, 125 × 10.0 mm (*Macherey & Nagel*); *A*: 20 mM KH_2PO_4 in H_2O/MeCN 4:1, pH 6.0; *B*: *A* + 1M KCl; flow 3 ml/min; detection 260 nm.

[c]) *Aquapore Rp-300*, 220 × 4.6 mm, 7 μm (*Brownlee Labs*); *A*: 0.1M (Et_3NH)OAc, in H_2O, pH 7.0; *B*: 0.1M (Et_3NH)OAc, in H_2O/MeCN 1:4, pH 7.0; flow 1 ml/min; detection 260 nm.

[d]) *Spherisorb-S10X RP-C18*, 10 μm, 300 Å, 220 × 12 mm; A: 0.1M (Et_3NH)OAc, in H_2O, pH 7.0; *B*: 0.1M (Et_3NH)OAc, in H_2O/MeCN 1:4, pH 7.0; flow 4 ml/min; detection 260 nm.

Reactions with Snake-Venom Phosphodiesterase. To 8–25 μM oligonucleotide in 1.25 ml of reaction buffer (180 mM NaCl, 12 mM *Tris* · HCl, pH 7.0) in a UV cell were added 5 ml (125 U) of alkaline phosphatase and 2 ml (6 mU) of snake-venom phosphodiesterase at 37°. The time courses of the reactions were followed by UV (260 nm) until constant UV absorption was reached.

X-Ray Structure of (3′S,5′R)-N⁴-Benzoyl-1-(2′-deoxy-3′,5′-ethano-α-D-ribofuranosyl)cytosine (**6**). Crystals were obtained as described in [13]: Cell parameters and space group were determined from precession photographs and from diffractometer measurements (least-squares fit of 14 reflections in the range $11 < \Theta < 14°$). The intensities of the reflections were measured at r.t. on a four-circle *Enraf-Nonius-CAD4* diffractometer with a graphite monochromator: $\lambda(MoK_\alpha) = 0.71069$ Å. During the measurement, two reflections were taken for intensity control every 10000 s; these showed no significant variation of the intensities. Two reflections were used for orientation control every 200 reflections. The intensities were corrected for *Lorentz* and polarization effects, but not for absorption. The structure was solved by direct methods with SHELXS-86 [27], and refined with SHELXS-76 [28] using $\sigma(F)^{-2}$ weights. Heavy atoms (C, O, N) were refined anisotropically. The positions of the H-atoms attached to the C-atoms were calculated and refined using constraints: H-atoms fixed at a distance of 1.08 Å, displacements parameters restricted to 120% of $(U_{11} + U_{22} + U_{33})/3$ of the corresponding C-atom. The position of the OH and NH H-atoms were determined from difference *Fourier* maps. They were refined with isotropic temperature factors; the OH H-atoms were fixed at a distance of 0.96 Å and the NH H-atoms at 1.02 Å. Crystal data (w = weighted refinement $(1/\sigma^2)$), see *Table 6*.

Table 6. *X-Ray Structure of* **6**

Formula	$C_{18}H_{19}N_3O_5$	Z	8
Space group	$P2_12_12_1$	d_x [g cm^{-3}]	1.33
Crystal system	orthorhombic	Θ max [°]	25
a [Å]	7.300(3)	Reflections unique	3339
b [Å]	18.88(1)	used ($I > 3\sigma(I)$)	2831
c [Å]	25.85(2)	R Factor	0.053
V [Å^3]	3562.5	R_w	0.052

REFERENCES

[1] M. Bolli, C. Leumann, *Angew. Chem.* **1995,** *34,* 694.

[2] M. Bolli, P. Lubini, M. Tarköy, C. Leumann, in 'Carbohydrates: Synthetic Methods and Applications in Antisense Therapeutics', Eds. Y.S. Sanghvi and P.D. Cook, ACS Symposium Series, Am. Chem. Soc., Washington, 1994, p. 100.

[3] M. Bolli, 'Nukleinsäure-Analoga mit konformationell eingeschränktem Zucker-Phosphat-Rückgrat ('Bicyclo-DNA'): Synthese und Eigenschaften', Diss. Universität Bern, 1994.

[4] U. Séquin, *Experientia* **1973,** *29,* 1059.

[5] F. Morvan, B. Rayner, J.-L. Imbach, M. Lee, J.A. Hartley, D.-K. Chang, J.W. Lown, *Nucleic Acids Res.* **1987,** *15,* 7027.

[6] G. Lancelot, J.-L. Guesnet, F. Vovelle, *Biochemistry* **1989,** *28,* 7871.

[7] F. Morvan, B. Rayner, J.-L. Imbach, D.-K. Chang, J.W. Lown, *Nucleic Acids Res.* **1987,** *15,* 4241.

[8] J. Paoletti, D. Bazile, F. Morvan, J.-L. Imbach, C. Paoletti, *Nucleic Acids Res.* **1989,** *17,* 2693.

[9] C. Cagnor, J. Bertrand, S. Thenet, M. Lemaitre, F. Morvan, B. Rayner, C. Malvy, B. Lebleu, J.-L. Imbach, C. Paoletti, *Nucleic Acids Res.* **1987,** *15,* 10419.

[10] F. Morvan, B. Rayner, J.-L. Imbach, S. Thenet, J.-R. Bertrand, J. Paoletti, C. Malvy, C. Paoletti, *Nucleic Acids Res.* **1987,** *15,* 3421.

[11] C. Gagnor, B. Rayner, J. Leonetti, J.-L. Imbach, B. Lebleu, *Nucleic Acids Res.* **1989,** *17,* 5107.

[12] J.S. Sun, C. Giovannangeli, J.-C. François, R. Kurfurst, T. Montenay-Garestier, U. Asseline, T. Saison-Behmoaras, N.T. Thuong, C. Hélène, *Proc. Natl. Acad. Sci. U.S.A.* **1991,** *88,* 6023.

[13] M. Tarköy, M. Bolli, B. Schweizer, C. Leumann, *Helv. Chim. Acta* **1993,** *76,* 481.

[14] M. Egli, P. Lubini, M. Bolli, M. Dobler, C. Leumann, *J. Am. Chem. Soc.* **1993,** *115,* 5855.

[15] M. Tarköy, M. Bolli, C. Leumann, *Helv. Chim. Acta* **1994,** *77,* 716.

[16] J. Hunziker, C. Leumann, in 'Modern Synthetic Methods', Eds. B. Ernst and C. Leumann, Verlag Helvetica Chimica Acta, Basel, 1995, p. 331–417.
[17] M. Tarköy, 'Nukleinsäure-Analoga mit konformationell eingeschränktem Zucker-Phosphat-Rückgrat (Bicyclo-DNS): Synthese und Eigenschaften Adenin- und Thyminhaltiger Bicyclooligonukleotide', Diss. ETH No. 10109, 1993.
[18] D. B. Davies, *Prog. NMR Spectrosc.* **1978,** *12,* 135.
[19] Y. Hayakawa, S. Wakabayashi, H. Kato, R. Noyori, *J. Am. Chem. Soc.* **1990,** *112,* 1691.
[20] U. Neidlein, C. Leumann, *Tetrahedron Lett.* **1992,** *33,* 8057.
[21] P. Job, *Anal. Chim. Acta* **1928,** *9,* 113.
[22] M. Durand, J.C. Maurizot, N.T. Thuong, C. Hélène, *Nucleic Acids Res.* **1988,** *16,* 5039.
[23] L.A. Marky, K.J. Breslauer, *Biopolymers* **1987,** *26,* 1601.
[24] G.S. Manning, *Q. Rev. Biophys.* **1978,** *11,* 179.
[25] M.T. Record, Jr., C.F. Anderson, T.M. Lohman, *Q. Rev. Biophys.* **1978,** *11,* 103.
[26] U. Pieles, W. Zürcher, M. Schär, H.E. Moser, *Nucleic Acids Res.* **1993,** *21,* 3191.
[27] G.M. Sheldrick, in 'Crystallographic Computing', Eds. G.M. Sheldrick, C. Krueger, and R. Goddard, Oxford University Press, Oxford, 1985.
[27] G.M. Sheldrick, 'System of Computing Programs', University of Cambridge, 1976.